

Strange dynamics of bilinear oscillator close to grazing

Ekaterina Pavlovskaja¹, James Ing¹, Soumitro Banerjee² and Marian Wiercigroch¹

¹ *Centre for Applied Dynamics Research, School of Engineering,*

King's College, Aberdeen University, Aberdeen, AB24 3UE, UK

E-mail: e.pavlovskaja@abdn.ac.uk, j.ing@abdn.ac.uk, m.wiercigroch@abdn.ac.uk

² *Department of Electrical Engineering, Indian Institute of Technology, India*

E-mail: soumitro.banerjee@gmail.com

Keywords: Impact Oscillator, Grazing Bifurcations, Chaos

SUMMARY. In this work strange behaviour of an impact oscillator with a one sided elastic constraint discovered experimentally [1, 2] is compared with the predictions obtained using its mathematical model. Particular attention is paid to the chaos recorded near grazing frequency when a non-impacting orbit becomes an impacting one under increasing excitation frequency. Extensive experimental investigations undertaken on the rig developed at the Aberdeen University [1, 3] reveal different bifurcation scenarios under varying excitation frequency near grazing which were recorded for a number of values of the excitation amplitude. It was found that the evolution of the attractor is governed by a complex interplay between smooth and non-smooth bifurcations. In some cases the occurrence of coexisting attractors is manifested through a discontinuous transition from one orbit to another through boundary crisis. One of those bifurcation scenarios is explained here based on numerical simulation.

1 INTRODUCTION

Simple piecewise systems have been studied extensively in the past. While much work has been devoted to finding normal forms and classifying the possible types of bifurcations in such systems, [4, 5, 6, 7] and references therein, comparatively little has been devoted to experimental verification of these, [3, 8, 9, 10, 11], and then only to a limited extent, or with simple rigid impact assumptions. This study presents detailed analysis of one of the bifurcation scenarios close to grazing in terms of the nonlinear bimodal maps that result from solving the linear equations in each subspace. The normal form 3/2 map resulting from grazing is often either the cause of or a direct precursor to a smooth bifurcation. Detailed simulations are shown to be in good correspondence with experiments both qualitatively and quantitatively.

1.1 *Experimental set up*

The experimental investigations were carried out on the impact oscillator [1, 2] shown in figure 1 which consists of a block of mild steel supported by parallel leaf springs providing the primary stiffness and preventing the mass from rotation. The secondary stiffness provided by an elastic beam is mounted on a separate column. Contact between the mass and the beam is made when their relative displacement is equal to zero. In practice, the contact is through a bolt which is attached to the beam. The length of the bolt can be adjusted to control the gap, g . The oscillator rig was mounted on an electro-dynamic shaker which provided harmonic excitation through the base. Displacement of the oscillator was measured with an eddy current probe displacement transducer mounted over one leaf spring. The acceleration of the oscillator was measured using an accelerometer mounted directly on the mass. A Savitzky-Golay algorithm was used to smooth the data, where a second

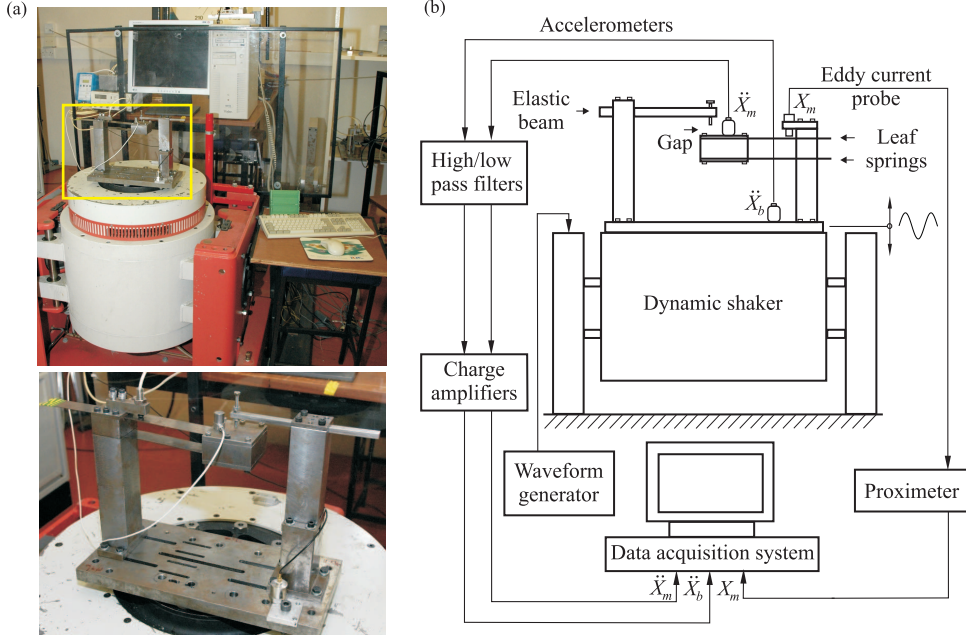


Figure 1: (a) Photographs of experimental setup. Parallel leaf springs prevent mass from rotation ensuring vertical displacement only. Harmonic excitation is provided to the oscillator from the shaker table. Since the oscillator mass is small when compared to the shaker armature, it is assumed that the oscillator does not interact with the shaker. (b) Schematic of experimental setup. Mass displacement, X_m , and accelerations of the mass and the base \ddot{X}_m , \ddot{X}_b are measured by an eddy current probe and two accelerometers respectively and then collected by the data acquisition system. [1]

order polynomial fitted to the eight surrounding data points gave the best results. The velocity was obtained from the smoothed displacement data.

1.2 Mathematical model

Simple model of the impact oscillator shown in figure 2a has been studied. A simplifying assumption that the discontinuity surface is not motion or time dependent, and is located at $x - e = 0$ has been made, and the equations of motion in the non-dimensional form [3, 12] are given below

$$\begin{aligned} x' &= v \\ v' &= a\omega^2 \sin(\omega\tau) - 2\xi v - x - \beta(x - e)H(x - e) \end{aligned} \quad (1)$$

where $x = y/y_0$ is the nondimensionalised displacement, $v = x'$ is the nondimensionalised velocity, $\tau = \omega_n t$ is the nondimensional time, $\beta = k_2/k_1$ is the stiffness ratio, $e = g/y_0$ is the nondimensional gap, $a = A/y_0$ is the nondimensional forcing amplitude, $\xi = c/2m\omega_n$ is the damping ratio, $y_0 = 1 \text{ mm}$ and $'$ denotes differentiation with respect to τ . Two resulting linear equations (different for contact and no contact modes) can be solved subject to initial conditions, and then maps P_1 and P_2 of these initial conditions between the two subspaces X_1 and X_2 produce the global response, see figure 2b. A periodic solution is found either by iterating the map, or, if a particular solution is

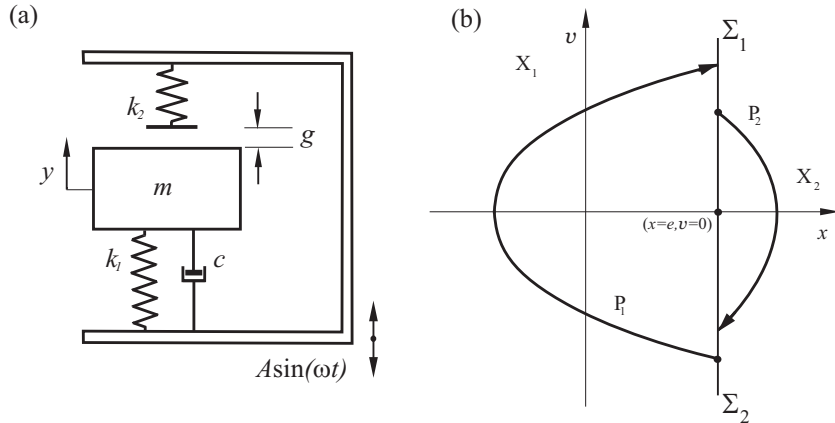


Figure 2: (a) Physical model of the oscillator. (b) Phase space is divided by the discontinuity boundaries Σ_1 and Σ_2 , and the locally valid maps P_1 and P_2 project the points from one boundary to another. [1]

being sought via the Newton method (once the Jacobian has been determined). The stability was analysed by finding the eigenvalues of the global Jacobian, constructed by composition from the local Jacobians in each subspace. Further details and explicit formulae can be found in [1].

2 NUMERICAL AND EXPERIMENTAL RESULTS

During the experimental study [1], a number of different bifurcation scenarios near grazing were recorded. The most typical one was when a non-impacting periodic orbit bifurcates into an impacting one via grazing mechanism. In some cases the resulting orbit is stable, but in most cases it loses stability through grazing. In those cases the appearance of the narrow band of chaotic behaviour was observed, and the example of such bifurcations is shown in figure 3a.

To investigate the recorded atypical bifurcation scenarios when close to grazing the non-impacting period-1 orbit bifurcates into chaotic regime, extended numerical simulations were conducted using the bi-linear oscillator described by Eqs.1. Very good correspondence between the theoretical predictions and the experimental results were obtained, explaining the experimentally observed phenomena. Figure 3 presents such correspondence showing the bifurcation diagrams with respect to frequency obtained experimentally and calculated numerically for one of the values of the excitation amplitude. As can be seen interesting bifurcation structure was recorded. Our detailed numerical simulations reveal that a number of co-existing attractors are present in the frequency region near grazing. Before grazing typically two orbits co-exist, one being a small non-impacting period-1 regime and the other one being a large amplitude impacting periodic regime. Figure 4 demonstrates the basins of attractions together with the corresponding trajectories of the co-existing non-impacting period-1 and impacting period-5 regimes found for the excitation amplitude $a = 0.7$ and frequency $\omega = 0.801$ just before the grazing. Here the basin of attraction for period-1 regime is shown in yellow and for period-5 regime – in orange.

When soon after grazing the stability of the small amplitude orbit is lost, the state could either move to the co-existing large amplitude orbit or in some cases to chaotic attractor composed of unstable manifolds of periodic orbits which are stable for higher excitation frequency values. For

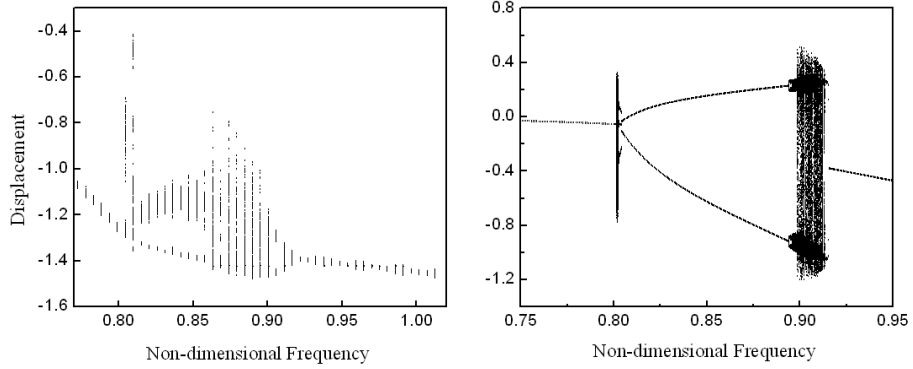


Figure 3: Bifurcation diagrams obtained (a) experimentally for excitation amplitude equal to 0.44 mm and (b) numerically for $a = 0.7$

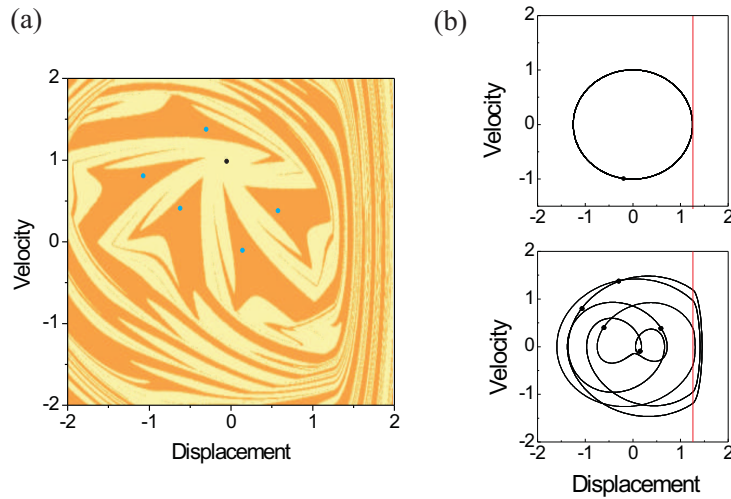


Figure 4: (a) Basin of attractions calculated for $a = 0.7$, $\omega = 0.801$, $g = 1.26$, $\xi = 0.01$, $\beta = 29$; (b) trajectories and Poincaré maps for the coexisting period-1 and period-5 solutions.

the considered case $a = 0.7$, while diverging away from the period-1 fixed point, when the state meets the unstable manifold of a period-3 point, the further iterates are constrained to remain on this unstable manifold. Thus, abruptly the unstable manifold of this period-3 fixed point becomes a stable attractor. Figure 5 shows the structural similarity between the unstable manifold of the period-3 saddle point (calculated using the *Dynamics* software [13]), and the chaotic orbit. As has been explained in [2], this narrow band chaotic orbit was possible due to the existence of the unstable period-3 orbits, which, in turn, was caused by the invisible grazing in the hard impact case or its smooth approximation in the soft impact case.

It has been shown in [2] that for the considered parameters set the two period-3 orbits which play a crucial role in forming the narrow band of chaos, are born at $\omega_1 = 0.7618806$ via a smooth saddle-

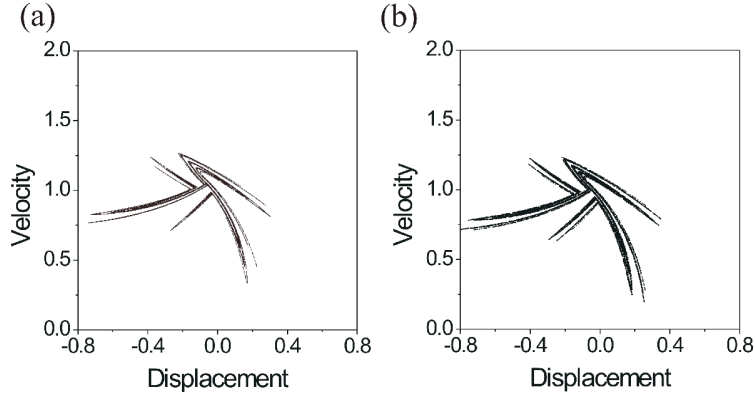


Figure 5: (a) Unstable manifold for period-3 attractor at $\omega = 0.802$ and (b) chaotic attractor at the same frequency. [2]

node bifurcation close to the point of invisible grazing. The bifurcations of these period-3 orbits were calculated as described in [1] and they are presented in figure 6. As can be seen the node (branch I) loses stability at $\omega = 0.761958$ through a period doubling bifurcation. The other unstable period-3 orbit (branch II) approaches the period-1 orbit as the grazing parameter value $\omega_{gr} = 0.801928$ is approached from below. Another unstable period-3 orbit (branch III in figure 6), born via a saddle node bifurcation at ω_2 , approaches from above. The close-up of the bifurcation diagram (figure 6b) shows two smooth saddle-node bifurcations occurring at very close parameter values, ω_3 and ω_4 , connecting unstable branches II and III with a stable period-3 orbit. Close to the grazing parameter value of ω_{gr} , the unstable period-3 orbit that forms the basin boundary comes very close to the periodic orbit. Thus, while in the nonsmooth approximation the distance between the fixed point and the unstable period-3 orbit is ideally zero at the bifurcation point [2], in the actual system there exists a very small but finite distance. If the ambient noise in the system (which is always present in a realistic situation) can perturb the state across the basin boundary, the state diverges away from the fixed point. Thus, even though the system is smooth in the ultimate analysis, a condition similar to that in dangerous border collision bifurcation is created.

The unstable period-3 orbit subsequently becomes stable through a reverse period doubling bifurcation (see the black portion in figure 6). This orbit and the unstable period-3 orbit created at ω_3 merge and disappear at a smooth saddle-node bifurcation at the parameter value ω_2 .

The presented analysis allows one to explain the appearance of the narrow band of chaos in the vicinity of the grazing. However the dynamics of the system in this frequency range is even more complex as other co-existing regimes were found as the frequency increases. Figure 7 demonstrates the basins of attractions for co-existing period-3 (in yellow), period-5 (in orange), period-8 (in brown) and period-2 (in dark brown) and the corresponding trajectories of these orbits found at $\omega = 0.8044$. As can be seen from this figure, the basins for period-2, period-3 and period-8 regimes are small and very fractal, and it is obvious that these attractors would not be robust in the presence of even small noise, which makes behaviour of the real system for those initial conditions highly unpredictable. It should be noted that some of those attractors exist only in a very narrow range of frequencies. For example, period-8 attractor shown in figure 7b has been found only for $\omega \in (0.8041, 0.8046)$ [14]. Further studies confirm that for the decreasing frequency a smooth period doubling bifurcation occurs at $\omega = 0.8041$ resulting in period-16 regimes with eight impacts.

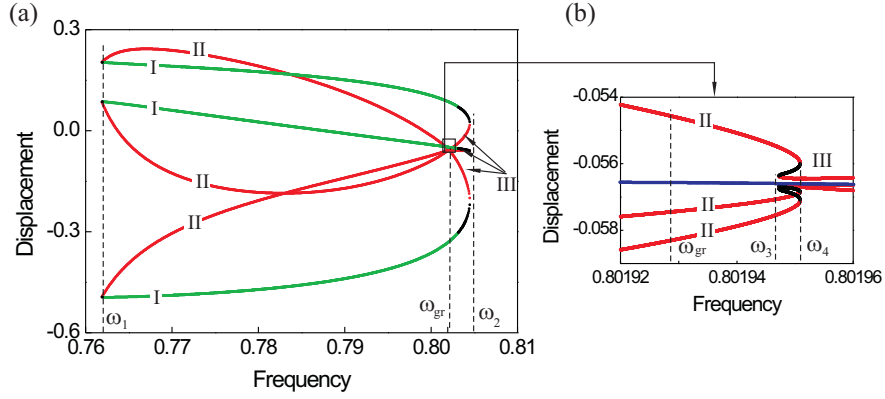


Figure 6: Bifurcation diagram showing the evolution of the period-1 and period-3 orbits in the soft impact system with stiffness ratio 29. The stable period-1 orbit is denoted by blue, stable period-3 orbits by black, and the two unstable period-3 orbits by red and green. [2]

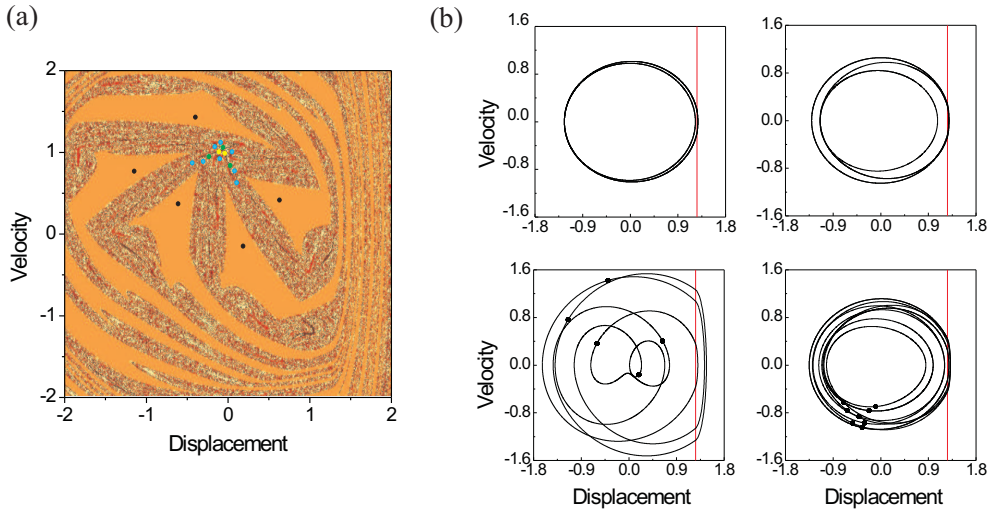


Figure 7: (a) Basin of attractions calculated for $a = 0.7$, $\omega = 0.8044$; (b) trajectories and Poincaré maps for the coexisting period-2, period-3, period-5 and period-8 solutions.

This is followed by a period doubling route to chaos, and the resulting chaotic attractor ceases to exist at $\omega \approx 0.80391$.

It has been demonstrated in [14] that in the frequency range shown in figure 3b a number of attractors co-exist, and among others the following combinations have been found: two different period-5 regimes and period-2 regime at $\omega \in (0.8056, 0.8062)$; various period-5 regimes (one at the time) and period-2 at $\omega \in (0.8062, 0.8066)$, $\omega \in (0.8067, 0.8296)$ and $\omega \in (0.8488, 0.8793)$;

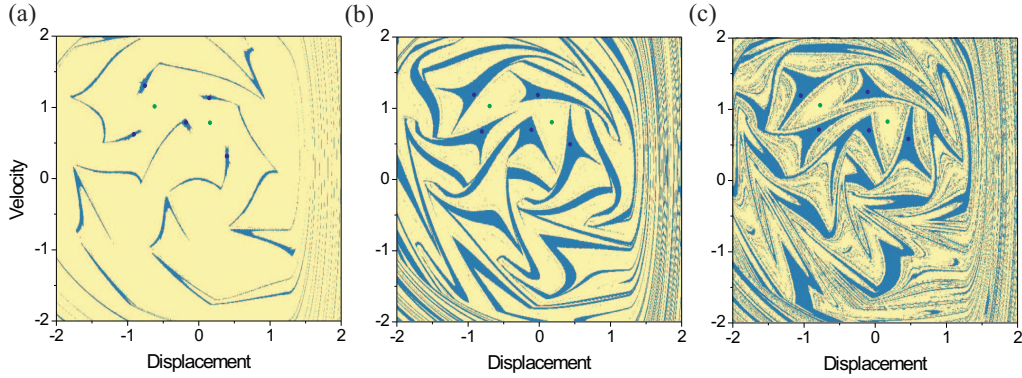


Figure 8: (a) Basin of attractions calculated for $a = 0.7$ and (a) $\omega = 0.85$; (b) $\omega = 0.86$; and (c) $\omega = 0.87$.

period-1 and period-3 regimes at $\omega \in (0.9257, 1.0491)$. Two, three or four different co-existing attractors were present at various frequency ranges and their basins of attractions were very fractal in some cases. Figure 8 presents the evolution of the basins for period-2 (in yellow) and period-5 (in blue) attractors co-existing at $\omega \in (0.8488, 0.8793)$.

3 CONCLUSIONS

The strange behaviour of an impact oscillator with a one sided elastic constraint has been demonstrated using the results of the bifurcation analysis. It has been shown that in the presented case as the system goes through grazing, non-impacting period-1 one orbit becomes impacting one, where the resulting impacting orbit loses stability and the system exhibits narrow band of chaos close to grazing. Following such an event, the evolution of the attractor is governed by a complex interplay between smooth and non-smooth bifurcations. The occurrence of coexisting attractors is manifested through discontinuous transition from one orbit to another through boundary crisis, which seems to be closely related to the grazing events. Simulations reveal that the coexisting attractors are often born far from the parameter values at which they are observed, but rapid cascades of period doubling and transitions to chaos result in the responses being unstable until another cascade brings them into play. So called invisible grazings result in the birth via saddle node bifurcation of orbits which are not stable for long enough to be observed, yet play a very important role in determining the dynamics by degrading the structural stability of coexisting attractors. Overall the correspondence between experiment and theoretical predictions are excellent and lend weight to various modelling assumptions used.

References

- [1] Ing, J., Pavlovskaja, E.E., Wiercigroch, M. and Banerjee, S., "Experimental study of impact oscillator with one sided elastic constraint", *Philosophical Transactions of the Royal Society* **366**(1866), 679–704 (2008).
- [2] Banerjee, S., Ing, J., Pavlovskaja, E.E., Wiercigroch M., and Reddy, R.K., "Invisible grazings and dangerous bifurcations in impacting systems: the problem of narrow-band chaos", *Physical*

Review E, **79**, 037201 (2009).

- [3] Wiercigroch, M. and Sin, V.W.T., "Experimental study of a symmetrical piecewise base-excited oscillator", *Journal of Applied Mechanics*, **65**, 657–663 (1998).
- [4] di Bernardo, M., Budd, C.J. and Champneys, A.R. "Normal-form maps for grazing bifurcations in n-dimensional piecewise smooth dynamical systems", *Physica D* **160**, 222–254 (2001).
- [5] Chin, W., Ott, E., Nusse, H.E. and Grebogi, C. "Grazing bifurcations in impact oscillators", *Phys. Rev. E* **50**, 4427–4444 (1994).
- [6] Di Bernardo, M. and Budd, C. J. and Champneys, A. R. "Grazing and border-collision in piecewise-smooth systems: a unified analytical framework", *Phys. Rev. Lett.* **86**, 2553–2556 (2001).
- [7] Ma, Y., Agarwal, M., and Banerjee, S. "Border collision bifurcations in a soft impact system", *Physics Letters A*, **354**(4), 281–287 (2006).
- [8] Ing, J., Pavlovskaia, E., and Wiercigroch, M. "Dynamics of a nearly symmetrical piecewise linear oscillator close to grazing incidence: Modelling and experimental verification", *Nonlinear Dynamics* **46**, 225–238 (2006).
- [9] Banerjee, S. and Grebogi, C. "Border collision bifurcations in two-dimensional piecewise smooth maps", *Phys. Rev. E* **59**, 4052–4061 (1999).
- [10] Todd, M.D. and Virgin, L.N. "An experimental impact oscillator", *Chaos, Solitons and Fractals* **8**, 699–715 (1997).
- [11] Wagg, D.J., Karpodinis, G. and Bishop, S.R. "An experimental study of the impulse response of a vibro-impacting cantilever beam", *Journal of Sound and Vibration* **228**, 243–264 (1999).
- [12] Shaw, S.W. and Holmes, P.J., "A periodically forced piecewise linear oscillator", *J. Sound and Vibration*, **90**(1), 129–155 (1983).
- [13] H. E. Nusse and J. A. Yorke, *Dynamics: Numerical Explorations*. Springer-Verlag, New York, (1998).
- [14] Ing, J. *Near grazing dynamics of piecewise linear oscillators*. PhD thesis, University of Aberdeen, (2008).